Simultaneous state-parameter estimation of rainfall-induced landslide displacement using data assimilation

Jing Wang[1], Guigen Nie[1,2], Shengjun Gao[3],Changhu Xue[1]

[1] GNSS Research Center, Wuhan University, Wuhan, 430079, China

[2] Collaborative Innovation Center for Geospatial Information Technology, Wuhan, 430079,China

[3] Chinese Antarctic Center of Surveying and Mapping, Wuhan, 430079, China

Corresponding to: Guigen Nie (ggnie@whu.edu.cn)

Abstract. Landslide displacement prediction has great practical engineering significance to landslide stability evaluation and early warning. The evolution of landslide is a complex dynamic process, applying a classical prediction method will result in significant error. Data assimilation method offers a new way to merge multi-source data with the model. However, data assimilation is still deficient in the ability to meet the demand of dynamic landslide systems. In this paper, simultaneous state-parameter estimation (SSPE) using particle filter-based data assimilation is applied to predict displacement of the landslide. Landslide SSPE assimilation strategy can make use of time-series displacements and hydrological information for the joint estimation of landslide displacement and model parameters, which can improve the performance considerably. We select Xishan Village, Sichuan province, China as experiment site to test SSPE assimilation strategy. Based on the comparison of actual monitoring data with prediction values, results strongly suggest the effectiveness and feasibility of SSPE assimilation strategy in short-term landslide displacement estimation.

1   Introduction

Landslide is a common geological hazard which greatly endangers the security of property and lives of the people (Huang et al., 2017; Froude M and Petley D, 2018; Zhang and Huang, 2018; Pham B T et al, 2018.). The landslide in Sri Lanka in May 2017 resulted in more than 200 casualties and injured 698,289 people. (Kumarasiri, 2018). In China alone, landslide hazards account for about 72.6% of the total geological disasters from 2005 to 2014(Xue et al., 2016). Therefore, landslides are important to study, leaning themselves for prevention studies like early warning systems and deformation predictions(Liu et al., 2014; Jiang et al., 2016; Michoud et al., 2016).

Landslide prediction and forecast methods have been developed and improved continually (Crosta et al., 2013; Li et al., 2018.). Chaussard E(2014) used the time-series analysis method applied to ALOS data to resolve land displacement in the Mexico region. Dong L (2012) proposed a model coupled Gray method and General Regression Neural Networks (GM-GRNN), and applied it to the prediction of sliding deformation of Dahu landslide. Li X Z (2014) carried out a genetic algorithm and support vector machine (GA–SVM) method to establish a mathematical function prediction model. Although the above

methods have certain practicability in the prediction of landslides, it is still problematic to carry out forecasts of rainfall-induced landslides in real time (Yin Y et al.2010). For the reason that surveillance photographs or optical remote-sensing satellites are not immediately available (Lee En-Jui,2019). It may take days, even months, to obtain field data and establish a process model of the study area. Moreover, most of the current model-based predictions cannot use the newest observation data effectively and therefore most likely deviate from the actual observations. The data assimilation method is a new technology that can help to overcome these challenges. By combining surface observational data with the process model, data assimilation provides an optimal "true value" that is continuously distributed over time and space (Xue C et al. 2018). Data assimilation has been widely tested and used in geoscience fields like hydrologic and atmospheric sciences (Reichle R H et al. 2002; Abbaszadeh P et al. 2017; Wikle C K et al. 2002). And although very promising, there have been only a few preliminary studies using data assimilation techniques that involves studying landslides.

Data assimilation can be divided into two types: the sequential-based method and the continuous-based method (Qin J et al. 2009). The sequential-based method is an online approach that updates the prediction each time (Nakano S. 2007), so it is more suitable for landslide systems than the continuous-based method. Particle Filter (PF) is a typical sequential data assimilation algorithm which was initially put forward by Gordon (Gordon N J et al. 2002). Because the PF is nonlinear filtering based on Bayesian estimation, it can solve non-linear and non-Gaussian problems (Moradkhani H et al. 2011). Landslides and parameters that describe landslides are typically non-linear (Leeuwen P J V. 2010), so we choose PF as the algorithm to integrate multi-source data with the model.

The evolution of a landslide is a time-varying process, so the model parameters are required to be adjusted over time. However, primal sequential data assimilation only updates state vectors, and the model parameters are generally given by known information, which will result in discrepancies between state and model parameters under a particular model relationship (Nearing G S et al., 2012). To meet the requirements of updating state values and model parameters simultaneously, we apply the simultaneous states and parameters estimation (SSPE) here. The SSPE method can continuously renewal the output by sequentially merging new measurements. Moradkhani H (2005) optimized this process in the hydrological field. Vrugt J A (2006) combined the simultaneous optimization with data assimilation. Joint estimation of state-parameter has proven to be a useful strategy to improve prediction performance (Qin J et al. 2009; Lü H et al. 2011).

In this paper, we applied the SSPE assimilation strategy to predict landslide displacement. In landslide SSPE assimilation, an external factor, hydrological data, has been integrated into the dynamic model of landslide deformation data, which can adjust model parameters and state vector simultaneously according to the hydrologic information. During the process, internal factors of a landslide are combined with external observation factors, and as such reducing the simulation error.

First, we will present the applied research method by describing the time-series decomposition, and how we established the model and landslide SSPE assimilation strategy applying the PF algorithm. The Xishan Village landslide is used here as study area to examine the SSPE assimilation strategy. The prediction of deformation will be optimized by coupling GPS observation data with a hydrological factor. Finally, we will present and discuss the results.

2 Method

2.1 Time-series displacement decomposition

Landslide deformation is the interaction between internal geological conditions and the external environment (Desai et al., 1995). Therefore the displacement can be divided into: a) a trend term displacement generated by inter factor, b) a periodic term displacement caused by external factors (such as rainfall and reservoir water level, etc.) and c) a stochastic term displacement (human impacted, snowpack, etc.)(Zhou C et al., 2016). However, after noise filtering, the stochastic term is too small and can be neglected. So the time-series displacement decomposition is as follows:

$$S(i) = \varphi(i) + x(i) \tag{1}$$

where $S(i)$ is the cumulative displacement of landslides, $\varphi(i)$ denotes the trend term, $x(i)$ denotes the periodic term.

The trend term of time series is extracted with the moving average method because it can remove the disturbance effectively and leave long-term signals for research (Seng H. 2014).

$$\varphi_i = \frac{S_{i-1} + S_{i-2} + \cdots S_{i-n}}{n} \tag{2}$$

where φ_i is the periodic term of step i, S_{i-1} is the cumulative displacement of step i-1, and n is the moving average period.

So the periodic term displacement can be calculated by subtracting the trend term from the total displacement.

2.2 Landslide periodic displacement modeling

For rainfall-induced landslides, atmospheric rainfall is one of the most susceptible disaster-causing factors and directly affects the periodic displacement of a landslide (Lian C et al., 2015; Ren F et al., 2015). So the periodic term can be regarded as a function of time and rainfall. The numerical function method is adopted here to establish a periodic displacement model. The periodic displacement variation is minimal for short periods of time. Therefore, the model can be derived through expanding periodic displacement value using a Taylor-series expansion method:

$$x(t_{i+1,}, r_{i+1}) = x(t_{i,}, r_i) + (\frac{\partial x}{\partial t})_{t_i}(t_{i+1} - t_i) + \frac{1}{2}(\frac{\partial^2 x}{\partial t^2})_{t_i}(t_{i+1} - t_i)^2 + (\frac{\partial x}{\partial r})_{r_i}(r_{i+1} - r_i) + \frac{1}{2}(\frac{\partial^2 x}{\partial r^2})_{r_i}(r_{i+1} - r_i)^2 + g_i \tag{3}$$

where x denotes displacement of the landslide, r_{i+1} is the rainfall of time i+1, $\frac{\partial x}{\partial t}$ and $\frac{\partial x}{\partial r}$ are the first order partial derivative of displacement, $\frac{\partial^2 x}{\partial t^2}$ and $\frac{\partial^2 x}{\partial r^2}$ are the second order partial derivative, g_i is the remainder of Taylor's expansion.

2.3 Landslide SSPE assimilation strategy using PF

2.3.1 State estimation

The general state-space model for a nonlinear dynamic system is defined to be:

State model: $x_{i+1} = f(x_i, u_i) + v_{i+1}$ (4)

Observation model: $y_{i+1} = g(x_{i+1}) + w_{i+1}$ (5)

where x is the state vector and y is the observation vector, i is a time step, f and g are nonlinear functions forecasting the state and observation, u represents the model parameters, v is the model error and w is observation noise.

2.3.2 Landslide SSPE method

In sequential data assimilation, SSPE algorithm can be applied through the state augmentation method (Chen T, 2005). Consider the model in Eq. (4), the original state vector x_i is now augmented with the parameters u(t) to be

$$X_i = \begin{bmatrix} x_i \\ u_i \end{bmatrix}$$ (6)

By incorporating the simultaneous state-parameter estimation method into the practical landslide state model Eq. (3), the extended state vector can be expressed as:

$$X_i = \left[x(t_i, r_i) \quad \left(\frac{\partial x}{\partial t}\right)_{t_i} \quad \left(\frac{\partial^2 x}{\partial t^2}\right)_{t_i} \quad \left(\frac{\partial x}{\partial r}\right)_{r_i} \quad \left(\frac{\partial^2 x}{\partial r^2}\right)_{r_i} \right]^T$$ (7)

And we set:

$$\left(\frac{\partial x}{\partial t}\right)_{t_{i+1}} = \left(\frac{\partial x}{\partial t}\right)_{t_i} + \left(\frac{\partial^2 x}{\partial t^2}\right)_{t_i}(t_{i+1} - t_i) + m_i$$ (8)

$$\left(\frac{\partial^2 x}{\partial t^2}\right)_{t_{i+1}} = \left(\frac{\partial^2 x}{\partial t^2}\right)_{t_i} + n_i$$ (9)

$$\left(\frac{\partial x}{\partial r}\right)_{r_{i+1}} = \left(\frac{\partial x}{\partial r}\right)_{r_i} + \left(\frac{\partial^2 x}{\partial r^2}\right)_{r_i}(r_{i+1} - r_i) + u_i$$ (10)

$$\left(\frac{\partial^2 x}{\partial r^2}\right)_{r_{i+1}} = \left(\frac{\partial^2 x}{\partial r^2}\right)_{r_i} + v_i$$ (11)

Where m_i、n_i、u_i、v_i are noise.

So the next moment X_{i+1} is:

$$X_{i+1} = \begin{bmatrix} x(t_{i+1}, r_{i+1}) \\ \left(\frac{\partial x}{\partial t}\right)_{t_{i+1}} \\ \left(\frac{\partial^2 x}{\partial t^2}\right)_{t_{i+1}} \\ \left(\frac{\partial x}{\partial r}\right)_{r_{i+1}} \\ \left(\frac{\partial^2 x}{\partial r^2}\right)_{r_{i+1}} \end{bmatrix} =$$

$$\begin{bmatrix} x(t_{i,},r_i) + (\frac{\partial x}{\partial t})_{t_i}(t_{i+1} - t_i) + \frac{1}{2}(\frac{\partial^2 x}{\partial t^2})_{t_i}(t_{i+1} - t_i)^2 + (\frac{\partial x}{\partial r})_{r_i}(r_{i+1} - r_i) + \frac{1}{2}(\frac{\partial^2 x}{\partial r^2})_{r_i}(r_{i+1} - r_i)^2 + g_i \\ (\frac{\partial x}{\partial t})_{t_i} + (\frac{\partial^2 x}{\partial t^2})_{t_i}(t_{i+1} - t_i) + m_i \\ (\frac{\partial^2 x}{\partial t^2})_{t_i} + n_i \\ (\frac{\partial x}{\partial r})_{r_i} + (\frac{\partial^2 x}{\partial r^2})_{r_i}(r_{i+1} - r_i) + u_i \\ (\frac{\partial^2 x}{\partial r^2})_{r_i} + v_i \end{bmatrix} =$$

$$\begin{bmatrix} 1 & t_{i+1}-t_i & \frac{1}{2}(t_{i+1}-t_i)^2 & r_{i+1}-r_i & \frac{1}{2}(r_{i+1}-r_i)^2 \\ 0 & 1 & t_{i+1}-t_i & 0 & 0 \\ 0 & 0 & 1 & 0 & 0 \\ 0 & 0 & 0 & 1 & r_{i+1}-r_i \\ 0 & 0 & 0 & 0 & 1 \end{bmatrix} \cdot \begin{bmatrix} x(t_{i,},r_i) \\ (\frac{\partial x}{\partial t})_{t_i} \\ (\frac{\partial^2 x}{\partial t^2})_{t_i} \\ (\frac{\partial x}{\partial r})_{r_i} \\ (\frac{\partial^2 x}{\partial r^2})_{r_i} \end{bmatrix} + \begin{bmatrix} g_i \\ m_i \\ n_i \\ u_i \\ v_i \end{bmatrix} =$$

$$\begin{bmatrix} 1 & t_{i+1}-t_i & \frac{1}{2}(t_{i+1}-t_i)^2 & r_{i+1}-r_i & \frac{1}{2}(r_{i+1}-r_i)^2 \\ 0 & 1 & t_{i+1}-t_i & 0 & 0 \\ 0 & 0 & 1 & 0 & 0 \\ 0 & 0 & 0 & 1 & r_{i+1}-r_i \\ 0 & 0 & 0 & 0 & 1 \end{bmatrix} \cdot X_i + \begin{bmatrix} g_i \\ m_i \\ n_i \\ u_i \\ v_i \end{bmatrix} \qquad (12)$$

In Eq. (12) we make $\begin{bmatrix} 1 & t_{i+1}-t_i & \frac{1}{2}(t_{i+1}-t_i)^2 & r_{i+1}-r_i & \frac{1}{2}(r_{i+1}-r_i)^2 \\ 0 & 1 & t_{i+1}-t_i & 0 & 0 \\ 0 & 0 & 1 & 0 & 0 \\ 0 & 0 & 0 & 1 & r_{i+1}-r_i \\ 0 & 0 & 0 & 0 & 1 \end{bmatrix} = \omega_{i+1}$, $\begin{bmatrix} g_i \\ m_i \\ n_i \\ u_i \\ v_i \end{bmatrix} = \varepsilon_{i+1}$, so Eq.(12) can be

expressed as:

$$X_{i+1} = \omega_{i+1} * X_i + \varepsilon_{i+1} \qquad (13)$$

The observation of landslide deformation can be expressed as:

$$y_{i+1} = x_i + w_{i+1} \qquad (14)$$

Combined the two expressions Eq. (13) and Eq. (14), we can build landslide SSPE state-space model to joint estimate

the landslide periodic displacement and model parameters.

2.3.3 PF algorithm

However, some parameters in the landslide state space model Eq. (13) and Eq. (14) are difficult to obtain (e.g.

$(\frac{\partial x}{\partial t})_{t_i}$, $(\frac{\partial^2 x}{\partial t^2})_{t_i}$). By applying Monte Carlo simulations, the PF can be adjusted to solve this. Instead of calculating partial

derivative directly, PF generates a large number of samples (particles) to approximate the posterior probability of the states,

thus obtaining an optimal result (Maskell and Gordon, 2002).

From Bayesian theorem, the posterior probability of the states can be inferred through

(1) forecast:

$$p(x_i|y_{1:i-1}) = \int p(x_i|x_{i-1}) \ p(x_{i-1}|y_{1:i-1})\mathrm{d}x_{i-1} \qquad (15)$$

(2) update:

$$p(x_i|y_{1:i}) = \frac{p(y_i|x_i)p(x_i|y_{1:i-1})}{p(y_i|y_{1:i-1})} \tag{16}$$

where i is time, x_i is the state vector, y_i is the observation vector, $y_{1:i} = \{y_1, y_2, \cdots, y_i\}$, $p(x_{i-1}|y_{1:i-1})$ is the posterior distribution function (PDF) for time step i-1, $p(x_i|y_{1:i-1})$ is the prior distribution for time step i, and $p(x_i|x_{i-1})$ can be derived from the model.

In PF, the posterior probability of the states are approximated by discrete random measures defined by particles and a set of weights associated with particles:

$$\hat{p}(x_i|y_{1:i}) \approx \sum_{k=1}^{N} w_i^k \, \delta(x_{0:i-}x_{0:i}^k) \tag{17}$$

where $\hat{p}(x_k|y_{1:k})$ is the approximate value of $p(x_k|y_{1:k})$, $x_{0:i}^k$ and w_k^i are particles and associated weight and $\sum_{i=1}^{N} w_k^i = 1$, and δ denotes Dirac delta function.

Direct sampling of target $p(x_k|y_{1:k})$ is can be problematic, so sequential importance sampling (SIS) is considered here to overcome this. The SIS gathers particles from a known density function and updates the importance weights by using an iterative method (Doucet A. et al. 2000). Meanwhile, the sampling importance resampling (SIR) is used to avoid particles deviate away from the truth value (Gordon N J et al. 2002). The SIR algorithm accumulate particles by their importance weight. So the estimates of the state vector can be described as:

$$\hat{x}_i = \sum_{k=1}^{N} x_i^k w_i^k \tag{18}$$

The procedure of landslide SSPE assimilation strategy is shown in Fig. 1.

3   Study area and data

3.1   Study area

Our study area is located in Xishan Village, Li County, Sichuan Province, China (Fig. 2), in the upper part of the left bank slope of the Zagunao River. The slope of this landslide is about 25° ~ 45°. The length is about 4200m, and the width is around 1700m. The altitude of the leading edge is 1500m, and the trailing edge is 3400m. Thus the elevation is 1900m. This landslide can be best described as a massive accumulative landslide. It can be divided into three parts according to the geomophogensis: (Ⅰ) erosional with a dip direction of about 178°; (Ⅱ) erosional and denudational with a dip direction of about 200°; (Ⅲ)Glacial and periglacial with a dip direction of about 208°. The distribution of the three parts are shown in Fig. 3. The Xishan landslide is a soft rock, layered structure slope. Exposed strata in the study area resembles mainly blue grey phyllite. The upper deposit is formed due to the collapse of slope and ice water accumulation and is mainly composed of silt and gravel soil.

Landform undulation leads to apparent local variations. Xishan Village landslide has a 52m thick active sliding layer which

can lead to about the movement of 85 million m³. Before 2008, many cracks appeared in the front and middle of this landslide, causing a direct economic loss of 0.5 million yuan and affecting 189 people. The creep deformation intensified after the Wenchuan earthquake (May 2008) which threatened the security of residents' lives and properties. The estimated potential economic loss was about 50 million yuan. For the purpose of reducing damage by providing early warning, this study was used to forecast the deformation of this landslide.

3.2 Data introduction

3.2.1 GPS derived time-series displacement

The Xishan Village landslide has been set up 5 GPS continuous observation stations for obtaining any deformation. The GPS receivers were connected to a network so the observations could be transferred in real time. At the same time, a GPS reference station was placed in a stable area and used for reference. Fig.3 shows the distribution of all stations. After the GPS baseline calculation, we calculated the deformation of every observation station from August 2015 to June 2017. Fig.4 shows the final results. Due to transmission problems, there are several gaps in the data. An interpolation method was applied to overcome these data gaps. (Velicer and Colby, 2005; Lenda G et al., 2016).

3.2.2 Rainfall data

There are two rain gauges on the landslide, which can transmit rainfall data in real time. Fig.3 shows the location of the rain gauges. Both are near GPS stations. The daily rainfall data is illustrated in Fig.6. Since the rain gauges are located near the GPS station, the mean values of the two gauges are taken as the rainfall of Xishan landslide.

4 Results and analysis

In this experiment, the performance of the proposed SSPE using particle filter-based data assimilation strategy is benchmarked with the SSPE method. The SSPE method only applied SSPE strategy and update state value with Eq.(13), without using data assimilation to optimize model and state parameters. All the experimental data was obtained at Xishan Village landslide between August 2015 and June 2017. We only present our findings for two stations GPS03 and GPS04 because the deformation is more evident there. Due to the complex terrain and insufficient power supply of Xishan Village, the monitoring GPS sequence had large error or noise. In order to reduce the influence of these, the time step is set to five days. The predicted displacement can be separated by a trend term, a period term and a cumulative term. Then the error analysis is taken to validate the efficiency of our method.

4.1 Prediction of trend term displacement

The trend term displacement is a time monotone function so that it can be fitted to a polynomial. The most optimal results of the trend term prediction and the fitting formula are shown in Fig. 5.

4.2 Prediction of period term displacement

The periodic term displacement can be calculated using the difference between the total displacement and the trend term. Fig. 6 shows the periodic displacement in station GPS03 and GPS04 and the rainfall data. It can be seen clearly that the period term is a complex nonlinear sequence series. Besides, fluctuation of the period term in two stations has the relatively same changing tendency, which is lagged behind that of rainfall. However, there are small differences in fluctuation like time step 40 to 50 and 70 to 76. This could be attributed to the impact of geology. The GPS04 station belongs to part Ⅰ. There are large numbers of people living here. The combined contribution of surface water, domestic water and ground water reduces the friction of the sliding belt, and thus leading to drastic distortion. The GPS03 station belongs to part Ⅲ. This part with rare plant cover is susceptible to heavy rainfall season.

We applied the SSPE assimilation method to predict periodic displacement. The prediction results are as shown in Fig. 7. It can be seen that the SSPE assimilation method get more close to the measured value than the SSPE method without assimilation.

4.3 Prediction of cumulative displacement

The predicted values of cumulative displacement can be obtained by summation of the predicted values of trend and periodic displacement. The prediction results for each station are shown in Fig. 8. Additionally, some detailed prediction data, differences between predicted and measured displacement and the error rates are enumerated in Table. 1 and 2. Experimental results verify the feasibility of SSPE assimilation method.

4.4 Relative error analysis

In this section, a more quantitative analysis is carried out to assess the performance of each method. Three criterions: Mean Absolute Error (MAE), Mean Squared Error (MSE) and Root Mean Square Error (RMSE) were used to evaluate the prediction effect. They can measure the deviation between the predicted value and the measured value, and are calculated by:

$$\text{MAE} = \frac{1}{N} * \sum_{i=1}^{N} |x_i - \hat{x}_i| \tag{19}$$

$$MSE = \frac{1}{N} * \sum_{i=1}^{N}(x_i - \hat{x}_i)^2 \tag{20}$$

$$RMSE = \sqrt{\frac{1}{N} * \sum_{i=1}^{N}(x_i - \hat{x}_i)^2} \tag{21}$$

Where x_i is the measured value and $\hat{x}_i$ is the prediction value.

The results are shown in Table. 3. According to the prediction evaluation indexes, SSPE assimilation method offers better forecast effect than the SSPE method. The MAE, MSE and RMSE value of SSPE assimilation method were 64.85%, 82.33% and 57.97% lower than those of SSPE method in GPS03 station respectively, and 6.66%,25.28% and 13.56% lower in GPS04 station respectively. The result suggests that the SSPE assimilation method has achieved great performance in landslide displacement prediction. Besides, the total execution time of two method is calculated. Building SSPE model for landslide displacement prediction only need 0.0048s and 0.0059s for the two stations, while the SSPE assimilation strategy takes 0.0844s and 0.0747s. It can therefore be considered as a near real-time solution to make displacement prediction simultaneously.

5   Conclusion

This paper presents a practical strategy on accurately predicting landslide displacement by coupling landslide deformation with external factors. For this, the PF data assimilation algorithm was integrated with the SPPE method. For the real data experiment, first the landslide deformation from GPS measurements were decomposed into a trend term and a period term. The period term was predicted with the hydrological factor in simultaneous estimation data assimilation, while the trend term was computed by polynomial fitting.

Our results show that SSPE assimilation strategy has an excellent ability for landslide displacement prediction and can provide assistance in early risk assessment and landslide forecasting.

Competing interests. The authors declare that they have no conflict of interest.

Acknowledgements: This study was financially supported by the National Program on Key Basic Research Project of China (grant numbers: 2013CB733205). Thanks to the editor and the anonymous reviewers. The authors acknowledge google earth for providing the map.

Reference:

Abbaszadeh P, Moradkhani H, Yan H.: Enhancing Hydrologic Data Assimilation by Evolutionary Particle Filter and Markov Chain Monte Carlo, Adv Water Resour, 111, 192-204, https://doi.org/10.1016/j.advwatres.2017.11.011, 2017.

Crosta G B, Frattini P, Agliardi F.: Deep seated gravitational slope deformations in the European Alps, Tectonophysics, 605, 13-33, https://doi.org/10.1016/j.tecto.2013.04.028, 2013.

Chaussard E, Wdowinski S, Cabral-Cano E, et al.: Land subsidence in central Mexico detected by ALOS InSAR time-series, Remote Sens Environ, 140, 94-106, https://doi.org/10.1016/j.rse.2013.08.038, 2014.

Chen T, Morris J, Martin E.: Particle filters for state and parameter estimation in batch processes, J Process Contr, 15(6), 665-673, doi:10.1016/j.jprocont.2005.01.001, 2005.

5   Desai C S, Samtani N C, Vulliet L.: Constitutive Modeling and Analysis of Creeping Slopes, Journal of Geotechnical Engineering, 122(6), doi:10.1061/(ASCE)0733-9410(1995)121:1(43), 1995.

Dong L, Li X.: An Application of Grey-General Regression Neural Network for Predicting Landslide Deformation of Dahu Mine in China, J Comput Theor Nanos, 6(1), 577-581, doi: 10.1166/asl.2012.2253, 2012.

Doucet, A., Godsill, S., & Andrieu, C.: On sequential monte carlo sampling methods for bayesian filtering. Statist and Comput,
10   10(3), 197-208, https://doi.org/10.1023/A:1008935410038, 2000.

Froude M, Petley D: Global fatal landslide occurrence from 2004 to 2016. Nat Hazards Earth Syst Sci, 18, 2161–2181, https://doi.org/10.5194/nhess-18-2161-2018 , 2018.

Gordon N J, Salmond D J, Smith A F M.: Novel approach to nonlinear/non-Gaussian Bayesian state estimation. IEE Proceedings F-Radar and Signal Processing, 140, 107-113, doi: 10.1049/ip-f-2.1993.0015, 2002.

15   Huang F, Huang J, Jiang S et al.: Landslide displacement prediction based on multivariate chaotic model and extreme learning machine, Eng Geol, 218, 173-186, https://doi.org/10.1016/j.enggeo.2017.01.016, 2017.

Jiang Y N, Liao M S, Zhou Z W et al.: Landslide Deformation Analysis by Coupling Deformation Time Series from SAR Data with Hydrological Factors through Data Assimilation, Remote Sens, 8, 179, https://doi.org/10.3390/rs8030179, 2016.

Kumarasiri W.K.: Damage and loss assessment of Landslide Disasters in Sri Lanka - A case study based on Landslide Disasters
20   in May 2017, in: Proceedings of the 8th Annual NBRO Symposium, At Colombo, Sri Lanka, January 2018, 2018.

Lee En-Jui, Liao Wu-Yu, Lin, Guan-Wei et al.: Towards Automated Real-Time Detection and Location of Large-Scale Landslides through Seismic Waveform Back Projection. Geofluids. 1, 1-14. doi:10.1155/2019/1426019. 2019.

Leeuwen P J V.: Nonlinear data assimilation in geosciences: an extremely efficient particle filter, Q J Roy Meteor Soc, 136(653), 1991-1999, doi: 10.1002/qj.699, 2010.

25   Lenda G, Ligas M, Lewińska P, et al.: The use of surface interpolation methods for landslides monitoring, Ksce J Civ Eng, 20, 188-196, https://doi.org/10.1007/s12205-015-0038-4, 2016.

Li H, Xu Q, He Y, et al.: Prediction of landslide displacement with an ensemble-based extreme learning machine and copula models, Landslides, 15, 2047–2059, https://doi.org/10.1007/s10346-018-1020-2, 2018.

Li X Z, Kong J M.: Application of GA-SVM method with parameter optimization for landslide development prediction, Nat

Hazard Earth Sys Sci, 14, 5295-5322, https://doi.org/10.5194/nhess-14-525-2014, 2014.

Lian C, Zeng Z, Yao W et al.: Multiple neural networks switched prediction for landslide displacement, Eng Geol, 186, 91-99, https://doi.org/10.1016/j.enggeo.2014.11.014, 2015.

Lü H, Yu Z, Zhu Y, et al.: Dual state-parameter estimation of root zone soil moisture by optimal parameter estimation and extended Kalman filter data assimilation, Adv Water Resour, 34, 395-406, https://doi.org/10.1016/j.advwatres.2010.12.005, 2011.

Liu Z, Shao J, Xu W, et al.: Comparison on landslide nonlinear displacement analysis and prediction with computational intelligence approaches. Landslides, 11, 889-896, https://doi.org/10.1007/s10346-013-0443-z, 2014.

Maskell S. and Gordon N.: A tutorial on particle filters for on-line non-linear/non-gaussian Bayesian tracking, IEEE T Signal Proces, 50, 174–188, doi:10.1049/ic:20010246, 2002.

Michoud C, Baumann V, Lauknes T R, et al.: Large slope deformations detection and monitoring along shores of the Potrerillos dam reservoir, Argentina, based on a small-baseline InSAR approach, Landslides, 13, 451-465, https://doi.org/10.1007/s10346-015-0583-4, 2016.

Moradkhani H, Sorooshian S, Gupta H V, et al.: Dual state–parameter estimation of hydrological models using ensemble Kalman filter, Adv Water Resour, 28, 135-147, https://doi.org/10.1016/j.advwatres.2004.09.002, 2005.

Moradkhani H, Weihermüller L.: Hydraulic parameter estimation by remotely—sensed top soil moisture observations with the particle filter, J Hydrol, 399, 410-421, https://doi.org/10.1016/j.jhydrol.2011.01.020, 2011.

Nakano, S., Ueno, G., and Higuchi, T.: Merging particle filter for sequential data assimilation, Nonlin. Processes Geophys., 14, 395-408, https://doi.org/10.5194/npg-14-395-2007, 2007.

Nearing G S, Crow W T, Thorp K R, et al.: Assimilating remote sensing observations of leaf area index and soil moisture for wheat yield estimates: An observing system simulation experiment, Water Resour Res, 48, 213-223, https://doi.org/10.1029/2011WR011420, 2012.

Pham B T, Tien Bui D, Prakash I.: Bagging based Support Vector Machines for spatial prediction of landslides. Environ Earth Sci, 77-146. https://doi.org/10.1007/s12665-018-7268-y, 2018.

Qin J, Liang S, Yang K, et al.: Simultaneous estimation of both soil moisture and model parameters using particle filtering method through the assimilation of microwave signal, J Geophys Res, 114(D15), https://doi.org/10.1029/2008JD011358, 2009.

Reichle R H, Mclaughlin D B, Entekhabi D.: Hydrologic Data Assimilation with the Ensemble Kalman Filter. Monthly Weather Review, 130,103-114, https://doi.org/10.1175/1520-0493(2002)130<0103:HDAWTE>2.0.CO;2, 2002

Ren F, Wu X, Zhang K et al.: Application of wavelet analysis and a particle swarm-optimized support vector machine to predict the displacement of the Shuping landslide in the Three Gorges, China, Environ Earth Sci, 73, 4791-4804, https://doi.org/10.1007/s12665-014-3764-x, 2015.

Seng H.: A new approach of moving average method in time series analysis. New Media Studies, 2014.

5   Velicer W.F. and Colby, S. M.: A Comparison of Missing-Data Procedures for Arima Time-Series Analysis, Educational & Psychological Measurement, 65, 596-615, https://doi.org/10.1177/0013164404272502, 2005.

Vrugt J A, Gupta H V, Nualláin B Ó et al.: Real-Time Data Assimilation for Operational Ensemble Streamflow Forecasting. J Hydrometeorol, 7, 548, https://doi.org/10.1175/JHM504.1, 2006.

Wikle C K.: Atmospheric Modeling, Data Assimilation, and Predictability, Technometrics, 47, 521-521, https://doi.org/10.1198/tech.2005.s326, 2002.

Xue, C., Nie, G., Li, H., and Wang, J.: Data assimilation with an improved particle filter and its application in the TRIGRS landslide model, Nat. Hazards Earth Syst. Sci., 18, 2801-2807, https://doi.org/10.5194/nhess-18-2801-2018, 2018.

Xue K, Yanxiang H U, Zou Y, et al.: Temporal-spatial distribution discipline of geological disaster in China in recent ten years. Chinese Journal of Geological Hazard & Control, 27, 90-97, doi:10.16031/j.cnki.issn.1003-8035.2016.03.14, 2016.

15   Yin Y, Wang H, Gao Y, et al.: Real-time monitoring and early warning of landslides at relocated Wushan Town, the Three Gorges Reservoir, China. Landslides, 7,339-349, doi: 10.1007/s10346-010-0220-1, 2010.

Zhang F, Huang X.: Trend and spatiotemporal distribution of fatal landslides triggered by non-seismic effects in China. Landslides, 15, 1663-1674, doi: 10.1007/s10346-018-1007-z, 2018.

Zhou C, Yin K , Cao Y , et al.: Application of Time Series Analysis and PSO-SVM Model in Predicting the Bazimen Landslide in the Three Gorges Reservoir, China, Eng Geol, 204, 108-120, https://doi.org/10.1016/j.enggeo.2016.02.009, 2016

25

30
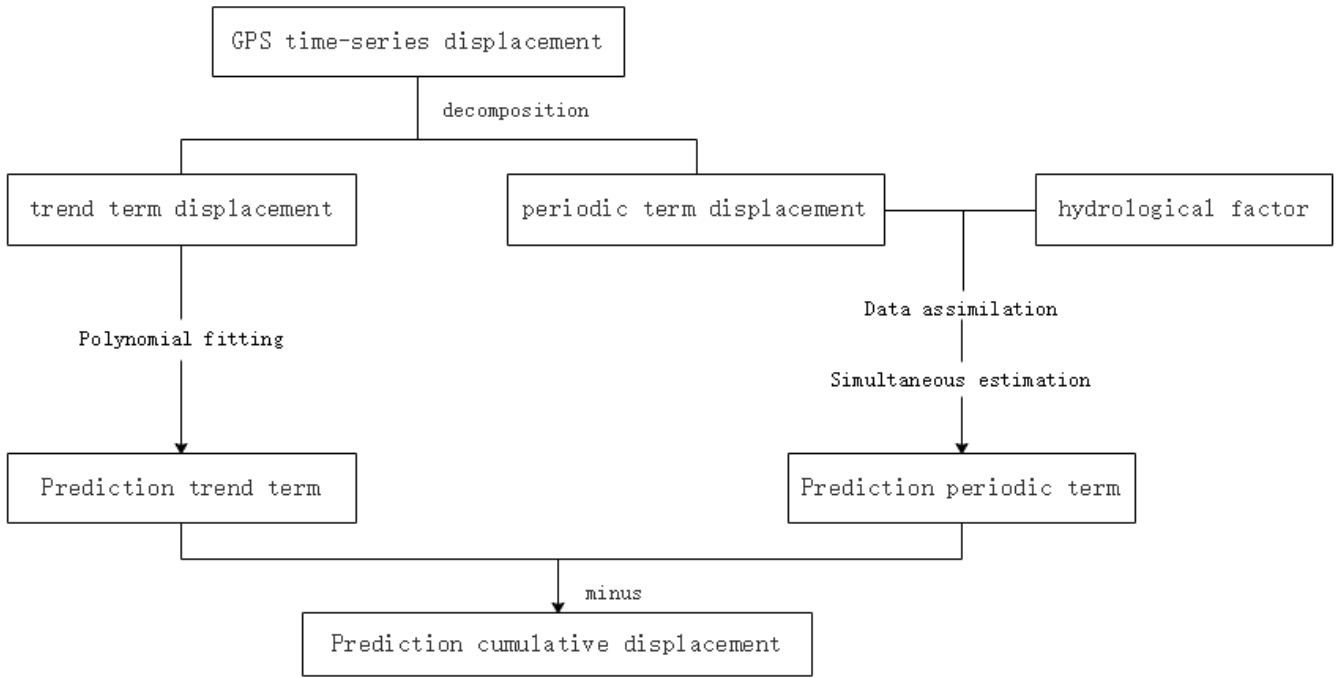
Figures

Figure 1. The flow chart of landslide SSPE assimilation strategy
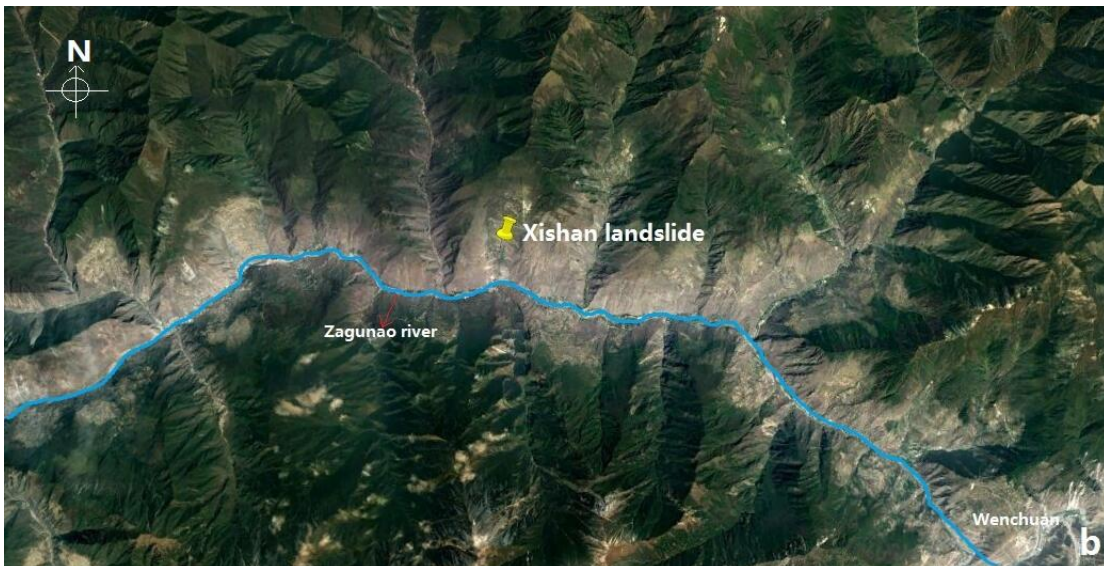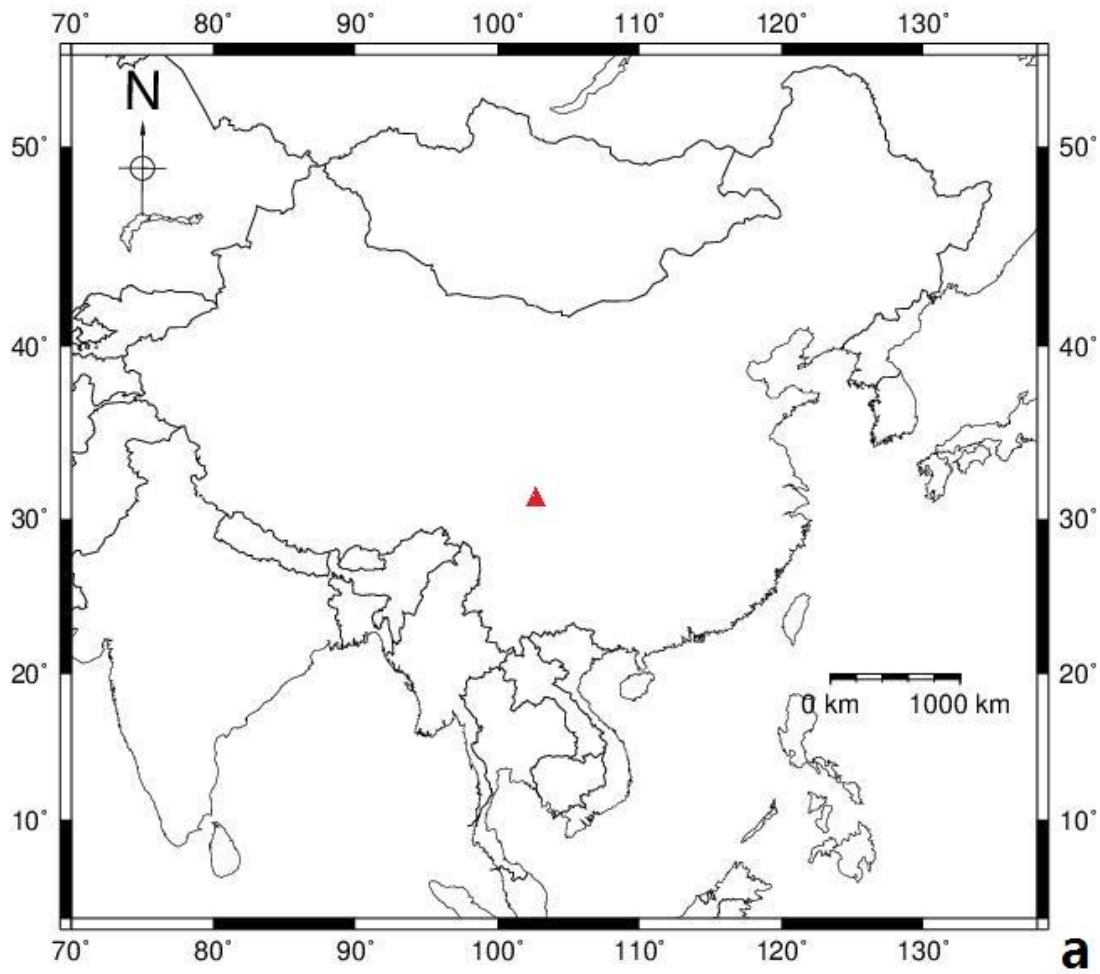
Figure 2. Location of the Xishan landslide in China (a); The Xishan landslides in the west of Wenchuan County associated with landform (b).
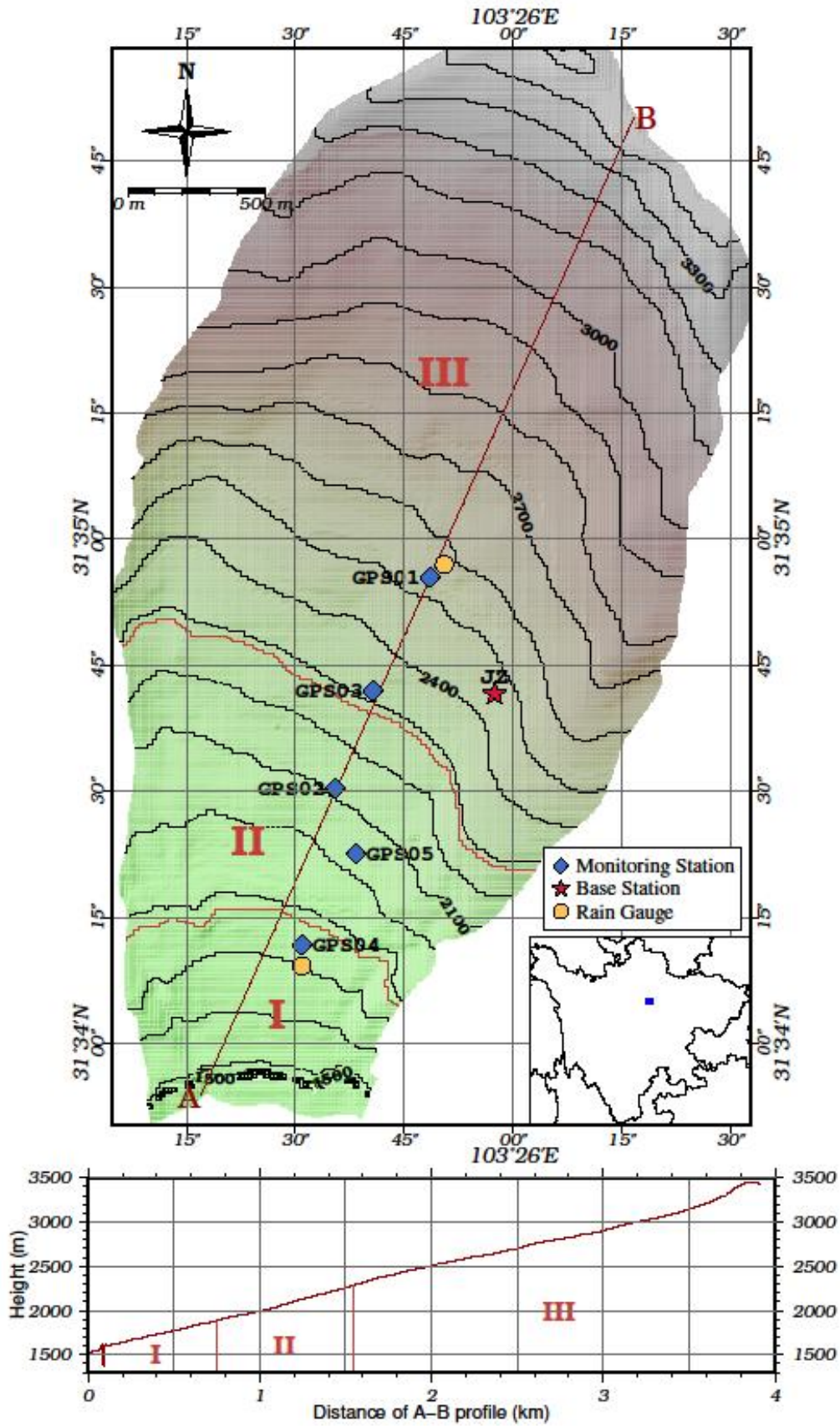
Figure 3. The distribution of three parts, GPS stations and rain gauges at Xishan landslide
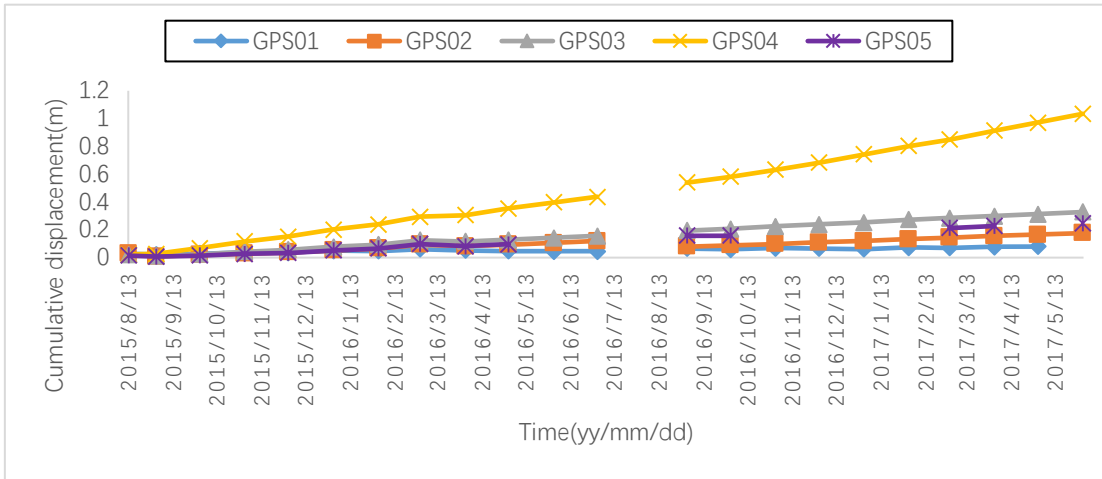
Figure 4. The GPS derived time-series displacement of Xishan landslide
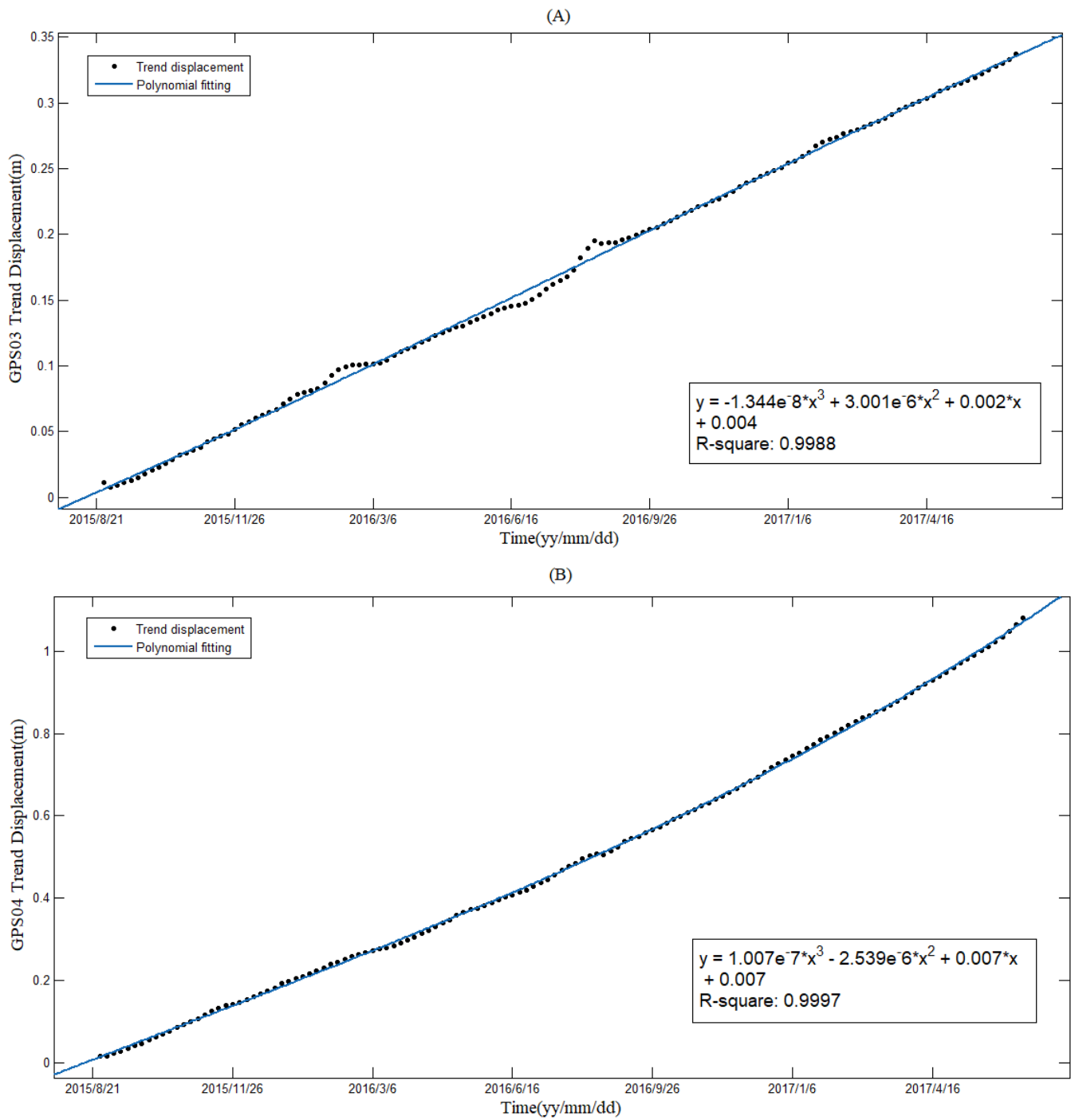
Figure 5. The trend term displacement prediction of (A)station GPS03, (B)station GPS04
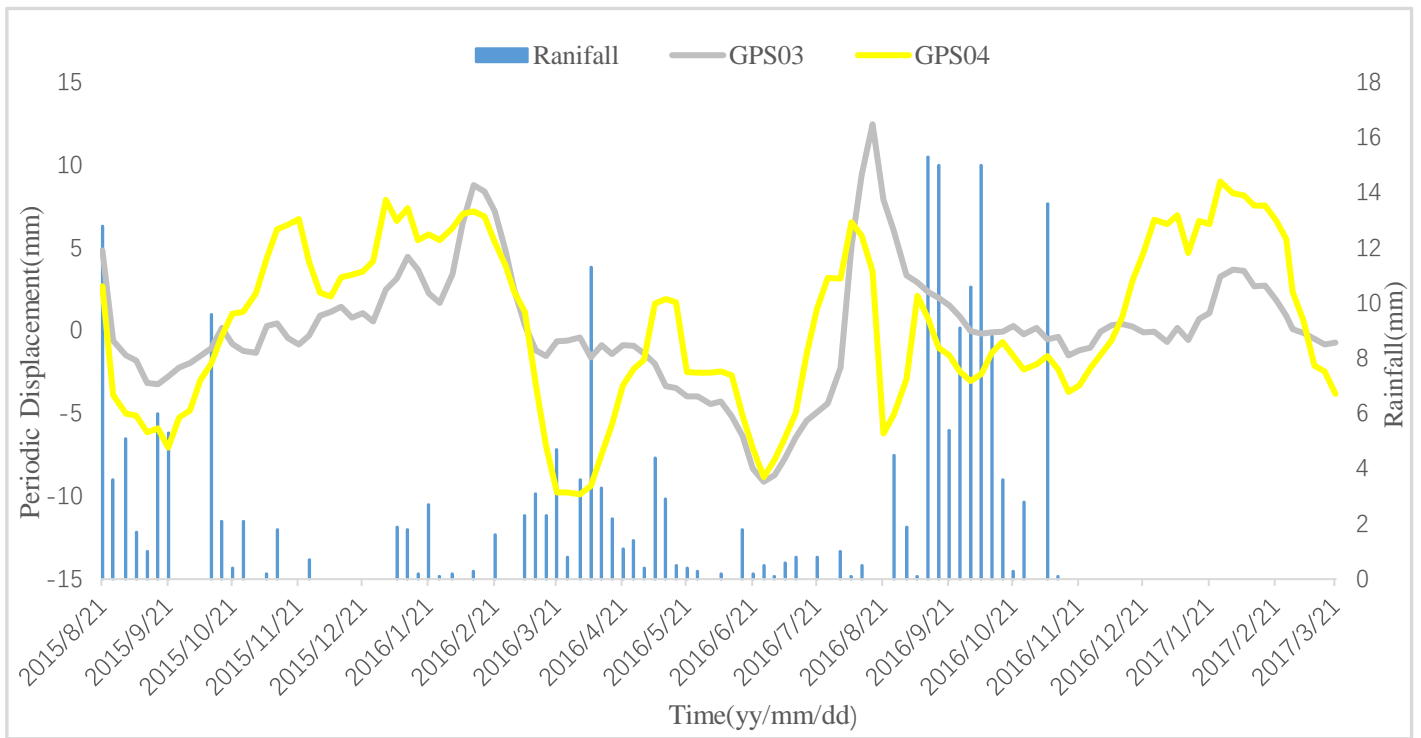
Figure 6. The periodic term displacement combined with rainfall data in GPS03 and GPS04
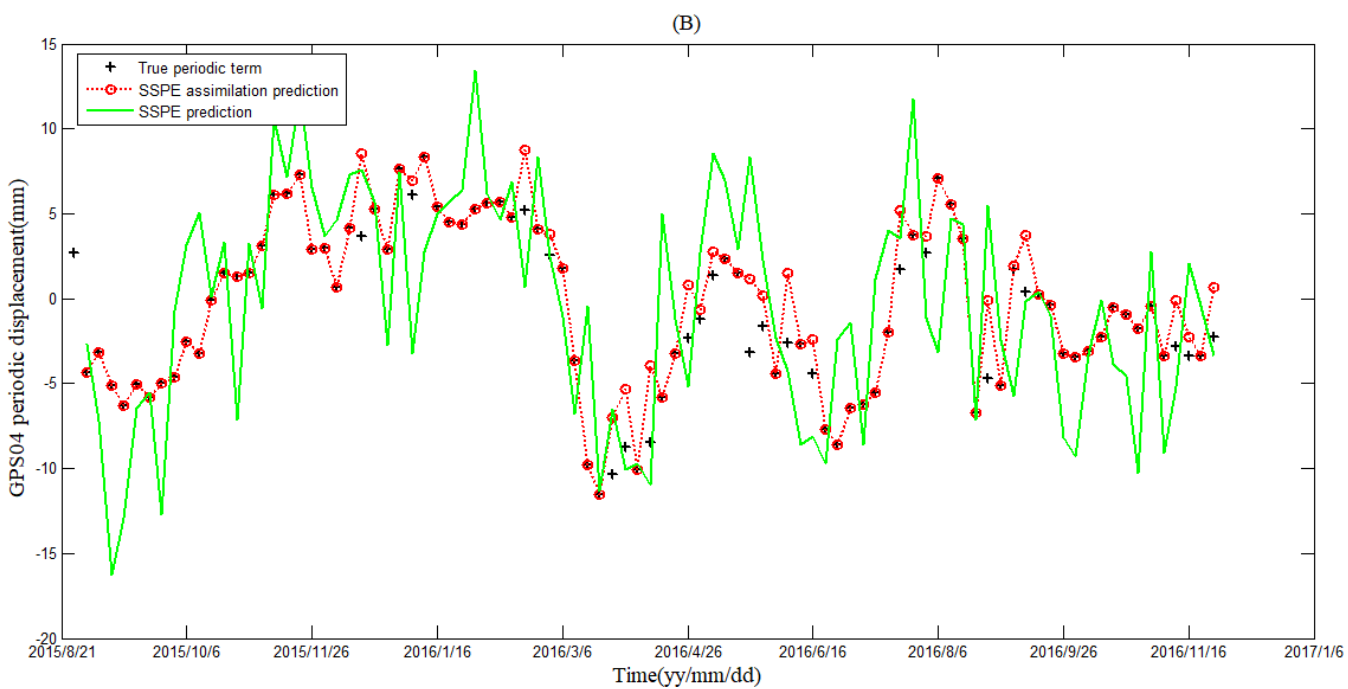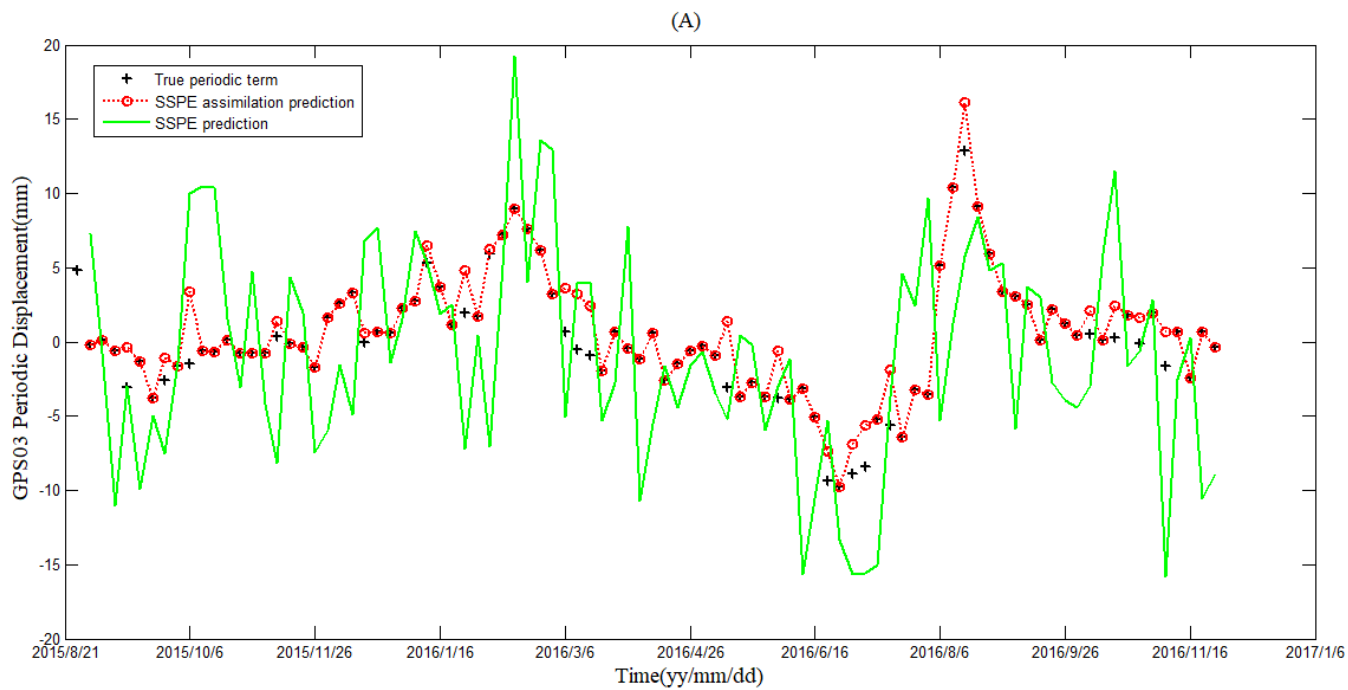
5   **Figure 7.** The periodic term displacement prediction of (A)station GPS03, (B)station GPS04
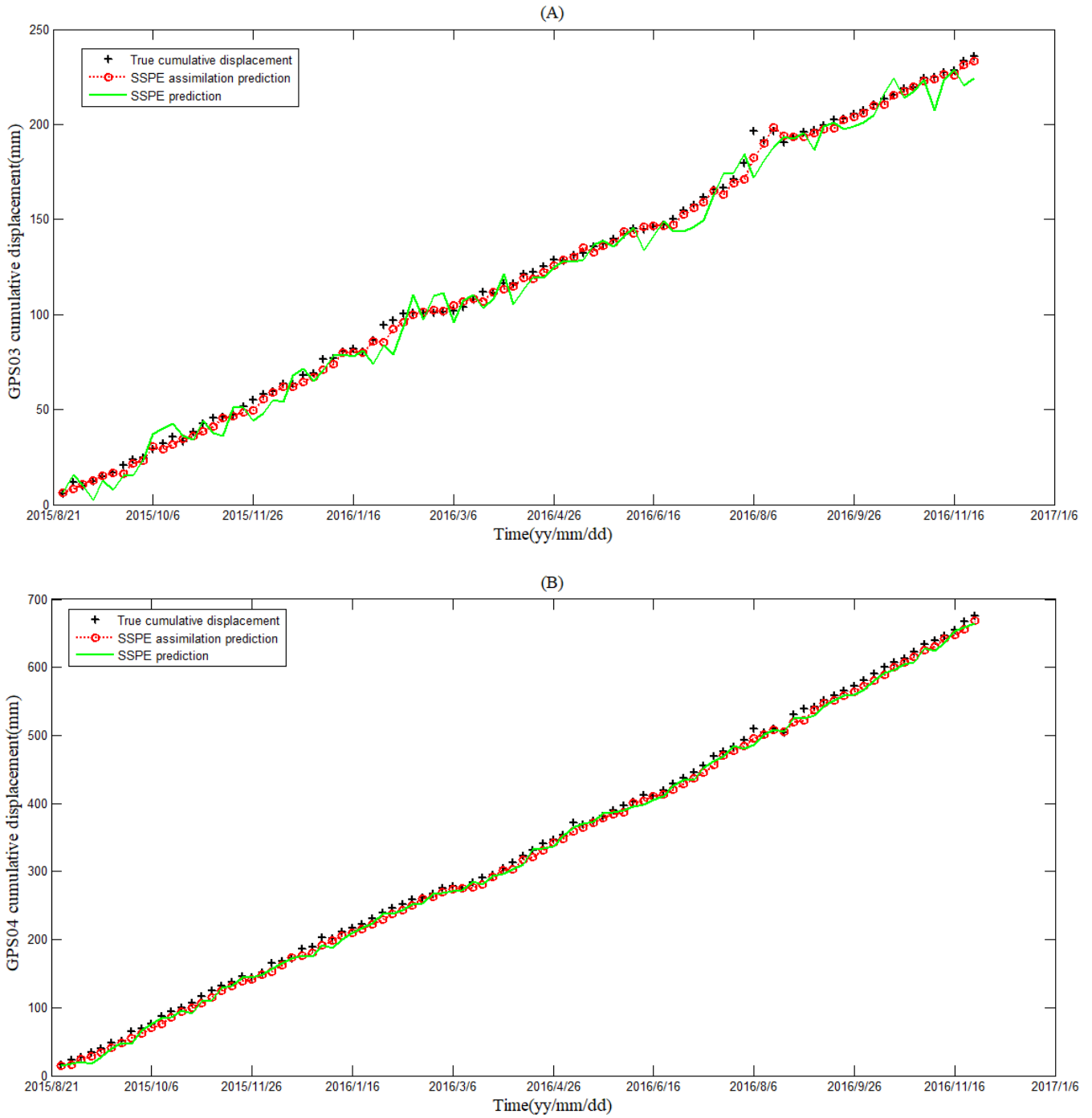
Figure 8. The cumulative displacement prediction of (A)station GPS03, (B)station GPS04

Tables

Table 1 Comparison between the predicted values of cumulative displacement and measured displacement using different methods in station GPS03

Time (yy/mm/dd)	Measured (mm)	SSPE			SSPE assimilation		
		Prediction (mm)	Difference (mm)	Error rate (%)	Prediction (mm)	Difference (mm)	Error rate (%)
2015/10/11	32.2674	40.2287	-7.9614	-24.67	29.1589	3.1085	9.63
2015/12/16	63.3499	68.1207	-4.7708	-7.53	61.8590	1.4909	2.35
2016/4/6	116.0395	105.4518	10.5878	9.12	115.0090	1.0305	0.89
2016/6/11	144.7729	133.5143	11.2586	7.78	145.9559	-1.1830	-0.82
2016/7/6	157.6520	146.3509	11.3011	7.16	156.2981	1.3539	0.86
2016/8/11	191.482	180.9944	10.4876	5.48	190.1751	1.3069	0.68
2016/10/16	215.3067	224.5674	-9.2607	-4.30	215.4657	-0.1590	-0.07
2016/11/21	233.1672	220.3506	12.8166	5.49	231.5734	1.5938	0.68

Table 2 Comparison between the predicted values of cumulative displacement and measured displacement using different methods in station GPS04

Time (yy/mm/dd)	Measured (mm)	SSPE			SSPE assimilation		
		Prediction (mm)	Difference (mm)	Error rate (%)	Prediction (mm)	Difference (mm)	Error rate (%)
2015/12/26	189.1781	175.2549	13.9232	7.36	180.9129	8.2652	4.37
2016/2/21	261.1626	252.4146	8.7480	3.35	260.5177	0.6449	0.25
2016/4/1	304.7420	296.5933	8.1486	2.67	301.3644	3.3775	1.11
2016/6/6	402.9618	394.7279	8.2339	2.04	400.5510	2.4108	0.60
2016/8/1	492.6282	479.9417	12.6865	2.58	484.7087	7.9195	1.61
2016/9/26	572.1082	559.3349	12.7733	2.23	564.2868	7.8214	1.37
2016/11/11	646.0208	636.9418	9.0790	1.41	642.0225	3.9983	0.62

Table 3. Comparison of MAE, MSE, RMSE performance and needed time using different methods in two stations

Method	MAE(mm)		MSE(mm)		RMSE(mm)		Execution time(s)	
	GPS03	GPS04	GPS03	GPS04	GPS03	GPS04	GPS03	GPS04
SSPE assimilation	2.2323	6.8323	9.5285	56.9071	3.0868	7.5437	0.0048	0.0059
SSPE	5.8533	7.3201	53.9320	76.1646	7.3438	8.7272	0.0844	0.0747